Removal of Acid Blue 40 from Aqueous Solution by Teak Leaf Litter Powder: Kinetics, Thermodynamics and Equilibrium Study

Emmanuel O. Oyelude[1,3*], Johannes A.M. Awudza[1], Sylvester K. Twumasi[2]

[1]*Department of Chemistry, Kwame Nkrumah University of Science and Technology, Kumasi, Ghana*
[2]*Faculty of Public Health, Catholic University College, Fiapre, Sunyani, Ghana*
[3]*Department of Applied Chemistry and Biochemistry, University for Development Studies, Tamale, Ghana*

Abstract

The equilibrium, kinetics and thermodynamics of the feasibility of using teak leaf litter powder (TLLP) to remove anionic Acid Blue 40 (AB40) dye from aqueous solution was investigated. Dye removal was influenced by contact time, TLLP dosage as well as concentration, pH and temperature of AB40 solution. Optimum removal of dye occurred at low TLLP dosage, acidic pH, and low dye concentration. Adsorption data fit well both Langmuir and Dubinin-Radushkevich isotherms and the maximum monolayer capacity of the adsorbent was 80.64 mg g^{-1} at pH 2 and 303 K. The kinetics of dye removal was best suited to the pseudo-second order model. The spontaneous and exothermic process was influenced by both intraparticle diffusion and liquid film diffusion but the latter was the rate-controlling step. The values of adsorption free energy (E), change in enthalpy ($\Delta H°$) and entropy ($\Delta S°$) were: 7.07 kJ mol^{-1}, -15.99 kJ mol^{-1} and -42.77 J mol^{-1} K^{-1}. TLLP may be a promising low-cost adsorbent for treating wastewaters containing AB40 and other anionic acid dyes.

1. Introduction

The textile industry produces the largest volume of colored wastewater containing residual dyes which must be safely treated before disposal or reuse.The challenges posed by the presence of dyes in water bodies include: degradation to produce carcinogenic by-products [1], slow biodegradation, stability to heat and irradiation, toxicity to aquatic organisms, obstruction of light penetration [2, 3] and inhibition of photosynthetic ability of aquatic plants [4].

Textile dyes may be broadly classified into three categories: cationic, anionic and non-ionic. C.I. Acid Blue 40 (AB40) is an anionic anthraquinone dye used for dyeing wool, silk and polyamide fibers [5]. Anthraquinone dyes exhibit diverse colors and their molecular structure makes them difficult to degrade [6].There are differs techniques employed for treating wastewaters containing dyes depending on the class of dye, severity of contamination, legislation, budget, efficiency and safety [7].The benefits and challenges of different treatment technology were discussed by Ashfaq and Khatoon [8].

The physicochemical technique of adsorptive removal of dyes from wastewater using activated carbon or graphene is widespread and the benefits of this technology have been documented [9, 10]. However, the adsorbents are expensive, possess poor selectivity properties and require costly regeneration before they can be reused [11]. Researchers are currently working to develop smart systems to address these demerits [12, 13]. Interfacial functionalized carbon nitride nanofibers have been prepared by hydrolyzing bulk carbon nitride in alkaline medium. The nanofibers were transformed into 3D hydrogel network and successfully applied to smart systems. The numerous advantages of these novel materials were reported by Zhang *et al*. [11]. However, they are yet to be available commercially to independently verify their effectiveness and cost.

The feasibility of employing agricultural materials and their by-products to treat dye-impacted wastewaters has been studied [14]. These materials are renewable, biodegradable, cheap and fairly effective [15] under laboratory conditions although most of them may require some modification to improve their adsorptive capacities. Some of the low-cost materials that have been studied for their feasibility to remove AB40 from

Oyelude et al., J. Mater. Environ. Sci., 2018, 9 (7), pp. 2087-2097

2087

aqueous solution include: *Thujaorientalis* biomass [14], surfactant modified barley straw [15], chemically modified barley straw [16] and *Punicagranatum L.* peels [17]. The calculated adsorption capacities of the four non-conventional adsorbents ranged from 51.95 to 138.10 mg g^{-1}, which compare well with that of granular activated carbon reported as 57.47 mg g^{-1} [18]. Teak leaf litter powder has already been reported as an effective adsorbent for removing eosin yellow dye from aqueous solution [19].

Teak, *Tectonagrandis Linn*, is a highly valued tropical hardwood indigenous to Asia [20]. It is planted as exotic species in plantations in West African countries of Ghana, Nigeria, Benin and Côte d'Ivoire [21]. The value chain analysis of teak focuses on its durable and attractive log which commands decent foreign exchange if exported [21-23]. The tree sheds its large broad leaves mainly during the dry season to produce enormous quantities of litter which may promote forest fire. Study conducted in Nigeria revealed that up to 9000 kg ha^{-1} of teak litter may be produced annually [24] which, presently, is largely unexploited economically.

This study focused on the practicality of employing readily available but disregarded teak leaf litter as a low-cost adsorbent for removing AB40 from aqueous solution. The study includes: characterisation of teak leaf litter powder, equilibrium adsorption, kinetics and thermodynamics. Selected isotherm models were used to fit the optimized equilibrium adsorption data and the monolayer capacity of the novel adsorbent was determined. The kinetic and thermodynamic experiments were conducted to clarify the type of adsorption and the rate controlling step in the uptake of the anionic dye by the adsorbent.

2. Material and Methods
2.1. Materials
A large quantity of teak leaf litter was sourced from the monoculture teak plantation on Navrongo Campus of University for Development Studies, Ghana. It was cleaned with large volume of tap water, rinsed with distilled water and air-dried. The crushed litter was washed clean with distilled water and oven-dried (Selecta, Barcelona, Spain) at 105°C for 8 h. The material was powdered, sieved to obtain average particle size below 210 μm and designated teak leaf litter powder (TLLP). Details about the characteristics of TLLP have been published [19].

All chemicals used were of analytical grade and used as received. 1000 mg L^{-1} stock solution of AB40 was prepared from which the experimental solutions (2-150 mg L^{-1}) were prepared as needed. Dilute dye of concentration ranging from 2 to 12 mg L^{-1} was used for linear calibration plot for determining the concentration of residual dye in solution after adsorption. 0.1 M HCl and 0.1 M NaOH solutions were used for pH adjustment.

2.2. Equilibrium Adsorption
Equilibrium adsorption experiments were carried out at 303 ± 1 K, except for the effect of temperature of dye solution. Fixed volume of AB40 solution was added to appropriate mass of TLLP in a stoppered Erlenmeyer flask and shaken on mechanical shaker (HS 260, Ika-Werk GMBH, Germany) at 120 rpm. Little quantity of dye solution was removed from the flask at predetermined time intervals and centrifuged (Selecta, Barcelona, Spain) at 2000 rpm for 5 min. The concentration of residual dye was obtained from the linear calibration plot after reading its absorbance at 518 nm using UV/visible spectrophotometer (Baloworld Scientific, England). The equations below were employed to determine the quantity of residual dye as R (%), q_t (mg g^{-1}) or q_e (mg g^{-1}).

$$R = \frac{(C_o - C_e) \times 100}{C_o} \quad (1)$$

$$q_t = \frac{(C_o - C_t)V}{w} \quad (2)$$

and

$$q_e = \frac{(C_o - C_e)V}{w} \quad (3)$$

where C_o (mg L^{-1}) is the concentration of AB40 before adsorption, C_t (mg L^{-1}) is the concentration at time, t (min), C_e (mg L^{-1}) is the equilibrium concentration of AB40, V (L) is the volume of AB40 and w (g) is the mass of TLLP. The mean of three replicate experiments with values within 5% of mean were recorded.

The effects of contact time and initial concentration of AB40 solution were conducted using 0.2 g of adsorbent and 100 mL of dye solution. The initial concentration of dye ranged from 25 to 75 mg L^{-1}. The influence of TLLP dosage was investigated by varying the initial mass of the adsorbent between 0.1 and 1.0 g. The volume and initial concentration of the dye were constant at 50 mL and 50 mg L^{-1}, respectively. The effect of pH on adsorption was investigated by varying the pH of AB40 solution between 1 and 11. However, the initial concentration and volume of dye as well as the mass of the adsorbent were constant at 50 mg L^{-1}, 50 mL and 0.2 g, respectively. The effect of temperature was examined between 298 and 313 K. The mass of adsorbent, initial concentration, volume and pH of AB40 were fixed.

2.3. Adsorption Isotherm

Experiments used to generate data for isotherm models were conducted by varying the concentration of AB40 from 25 to 150 mg L^{-1}. However, the mass of TLLP was 0.1 g while the volume, pH and temperature of the dye were: 100 mL, 2 and 303 ± 1 K, respectively. Langmuir isotherm [25], Scatchard isotherm [26], Freundlich isotherm [27] and Dubinin-Radushkevich isotherm [28] models were then used to fit the data. Langmuir isotherm assumes a homogeneous surface and constant adsorption potential. Its linear form is:

$$\frac{C_e}{q_e} = \frac{1}{q_m} C_e + \frac{1}{q_m} \frac{1}{C_e} \tag{4}$$

where C_e (mg L^{-1}) is the concentration of dye removed at equilibrium, q_e (mg g^{-1}) is the mass of dye removed at equilibrium per unit mass of adsorbent, q_m (mg g^{-1}) is the monolayer adsorption capacity of the adsorbent, and K_L (L mg^{-1}) is the Langmuir constant related to the rate of adsorption. The values of q_m and K_L were determined from the plot of C_e/q_e against C_e. The applicability of Langmuir model to adsorption was verified using separation factor, R_L, given by:

$$R_L = \frac{1}{1 + K_L C_o} \tag{5}$$

where K_L (L mg^{-1}) and C_o (mg L^{-1}) are the Langmuir adsorption constant and the highest initial concentration of AB40, respectively.

Scatchard isotherm is employed to obtain information about the type of interaction between the dye and the adsorbent. The linear equation is

$$\frac{q_e}{C_e} = q_m b - q_e b \tag{6}$$

where q_e (mol g^{-1}) and C_e (mol L^{-1}) are the equilibrium concentration of adsorbate on adsorbent and in solution, respectively; q_m (mol g^{-1}) is the maximum adsorption capacity and b (L mol^{-1}) is the adsorption binding constant. The values of q_m and b are obtained from the plot of q_e/C_e against q_e.

Freundlich isotherm assumes continuous or multilayer adsorption onto heterogeneous surface. The linear equation is

$$\log q_e = \frac{1}{n} \log C_e + \log K_F \tag{7}$$

where q_e (mg g^{-1}) is the mass of dye removed at equilibrium per unit mass of adsorbent, C_e (mg L^{-1}) is the concentration of dye removed at equilibrium, K_F (mg g^{-1})(L mg^{-1})$^{1/n}$ is a constant that represents the adsorbent capacity and dimensionless $1/n$ stands for the heterogeneity factor. The values of $1/n$ and K_F were determined from the plot of $\log q_e$ against $\log C_e$.

Dubinin-Radushkevich isotherm is general without assumption on the surface type of the adsorbent and the potential of adsorption. It is used to determine the mean free energy and nature of adsorption. Its linear form is:

$$\ln q_e = \ln q_{DR} - \beta \varepsilon^2 \tag{8}$$

where q_{DR} (mg g^{-1}) is the Dubinin-Radushkevich maximum monolayer adsorption capacity, β (mol^2 J^{-2}) is activity coefficient related to mean adsorption energy, and ε is the Polanyi potential which is calculated as follows

$$\varepsilon = RT \ln \left(1 + \frac{1}{C_e}\right) \tag{9}$$

where R (8.314 J mol^{-1} K^{-1}) is the gas constant, T (K) is temperature and C_e (mg L^{-1}) is the concentration of adsorbate at equilibrium. The values of q_{DR} and β were determined from the plot of $\ln q_e$ against ε^2. The mean free energy of adsorption, E (J mol^{-1}), is determined as follows

$$E = \frac{1}{\sqrt{2\beta}} \tag{10}$$

2.4. Adsorption Kinetics

The kinetics experiments were conducted at 303 ± 1 K using 0.2 g of TLLP and 100 mL AB40 solution at pH 2. The initial concentration of the dye solution was varied from 25 to 100 mg L^{-1}. The rate of removal of dye by the adsorbent was monitored as in the effect of initial dye concentration and contact time. The adsorption kinetic data was assessed using four models. The pseudo-first order kinetic [29, 30] is often applicable at the initial period of adsorption when the rate of uptake of adsorbate is fast. The linear equation is

$$\log(q_e - q_t) = \log q_e - k_1 t \tag{11}$$

where, q_e (mg g^{-1}) and q_t (mg g^{-1}) are the quantity of dye removed at equilibrium and time, t (min), respectively; and k_1 (min^{-1}) is the pseudo-first order rate constant. The values of k_1 and q_e were determined from the plot of $\log(q_e-q_t)$ against t.
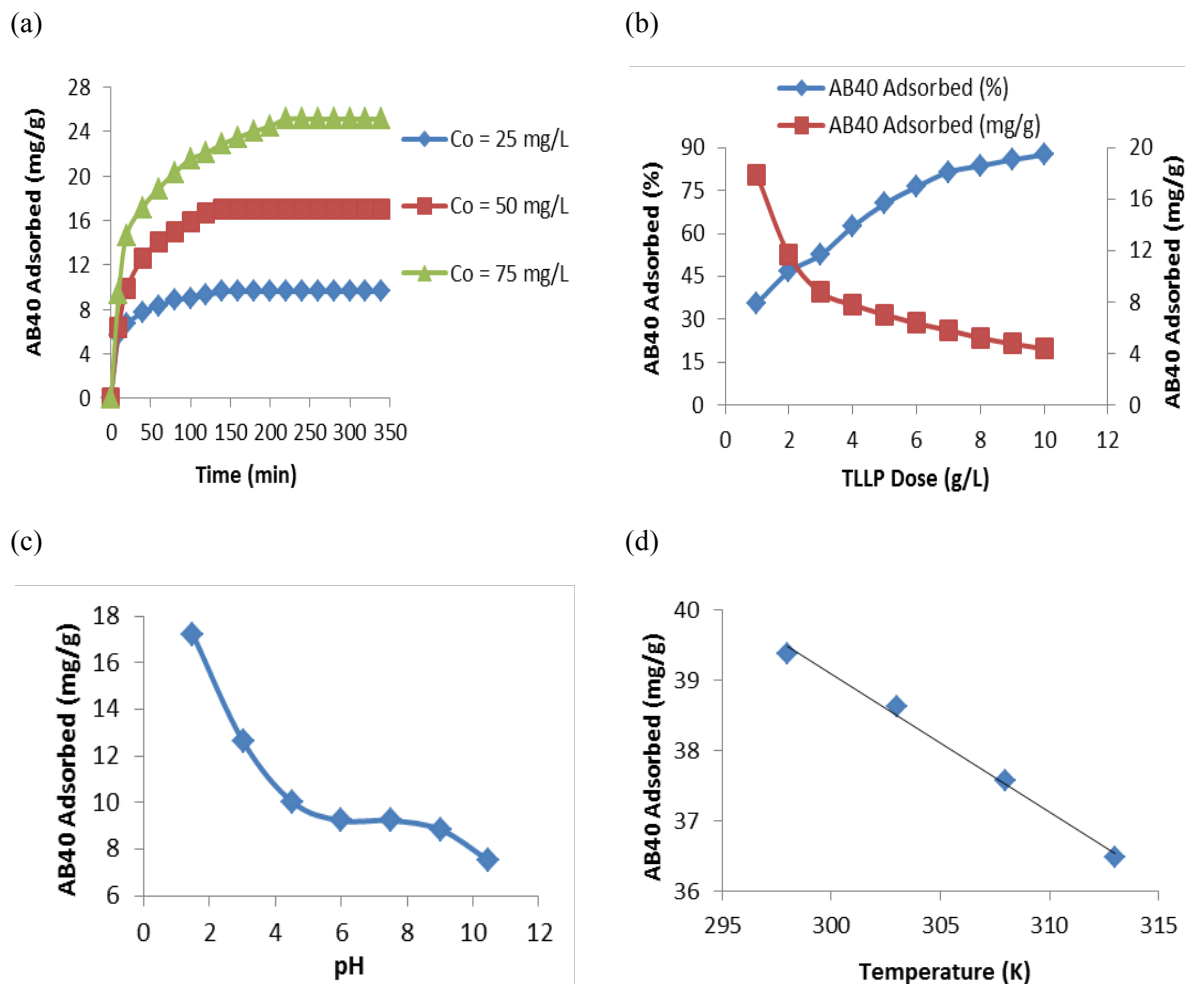
Figure 1: Effect of concentration of dye and contact time (a), dose of TLLP (b), pH of AB40 solution (c) and temperature (d) on removal of AB40 from aqueous solution by TLLP

The pseudo-second order equation [31] tends to be applicable over the entire duration of an adsorption process. The equation is

$$\frac{t}{q_t} = \frac{1}{k_2 q_e^2} + \frac{1}{q_e} t \tag{12}$$

where, q_t (mg g^{-1}), q_e (mg g^{-1}) and t (min) are as defined earlier and k_2 (g mg^{-1} min^{-1}) is the pseudo-second order rate constant. The values of q_e and k_2 were determined from the plot of t/q_t against t. The value of k_2 is normally inversely proportional to the initial concentration of adsorbate. The initial rate of adsorption, h, is calculated from the following equation

$$h = k_2 q_e^2 \tag{13}$$

The intraparticle diffusion kinetic [32] plays a role influencing the mechanism of adsorption [33]. It considers the movement of adsorbate molecules or ions from the surface into the pores of an adsorbent. Its equation is

$$q_t = k_{id} t^{1/2} + C \tag{14}$$

where, q_t (mg g^{-1}) and t (min) are as earlier defined, k_{id} (mg g^{-1} min$^{-1/2}$) is the intraparticle diffusion rate constant and C is a constant pertaining to boundary layer. The values of k_{id} and C were obtained from the plot of q_t against $t^{1/2}$.

The Boyd equation [34] was applied to aid in the clarification of the rate controlling stage of the adsorption mechanism. It considers the movement of adsorbate molecules or ions from bulk solution through the liquid film surrounding the adsorbent. The equation is

$$F = 1 - \left(6 / \pi^2\right) e^{\left(-Bt\right)} \tag{15}$$

where, $F = q_t/q_e$, is the level of equilibrium attained at time t (min). Bt is a function of F and can be approximated using the expression

$$Bt = -0.4977 - \ln\left(1 - F\right) \tag{16}$$

Oyelude et al., J. Mater. Environ. Sci., 2018, 9 (7), pp. 2087-2097

2090
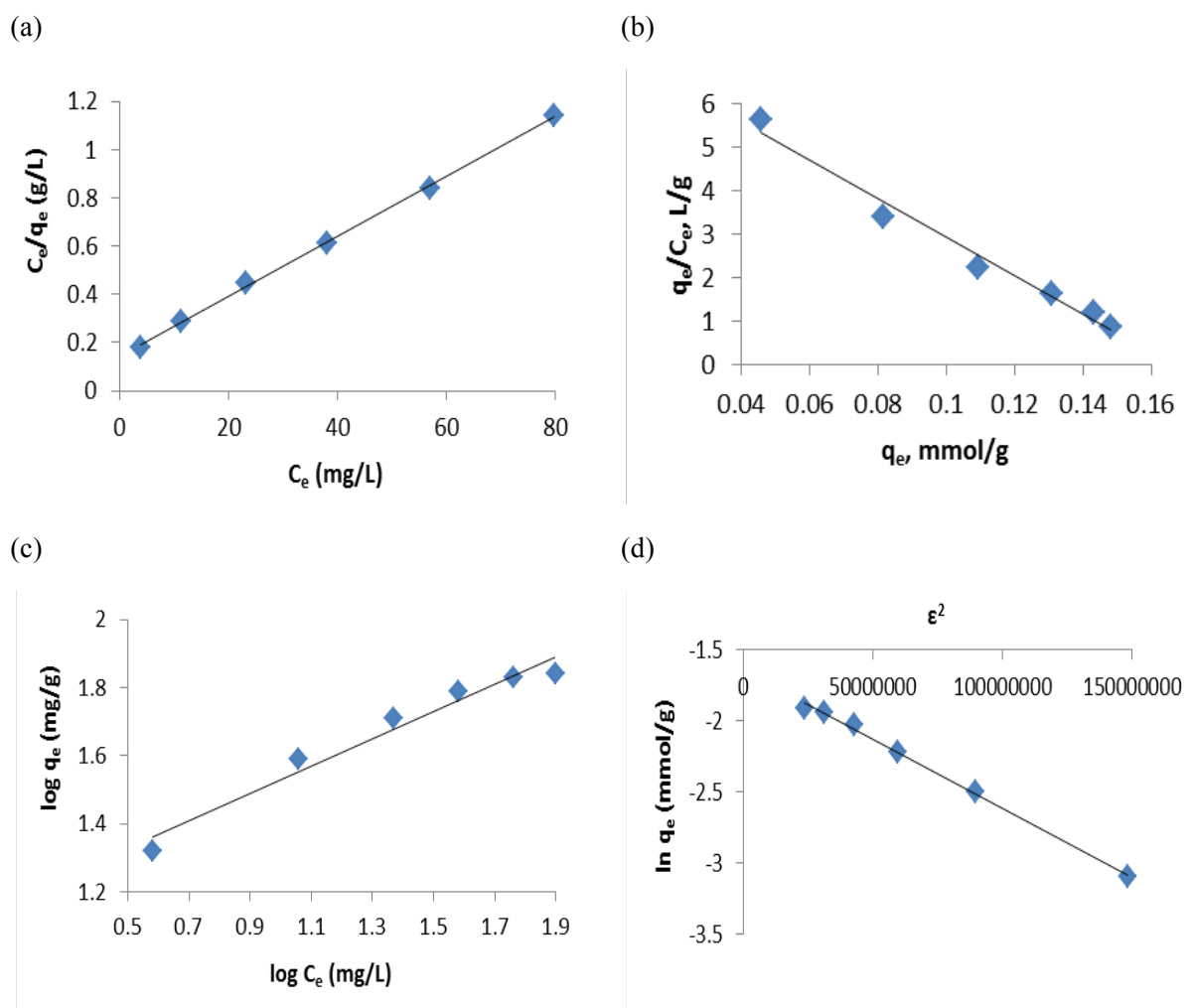
Figure 2: Linear plots of Langmuir (a), Scatchard (b), Freundlich (c) and Dubinin-Radushkevich (d) isotherms for removal of AB40 by TLLP

2.5. Adsorption Thermodynamics

The thermodynamic experiments were similar to those on the effect of temperature described earlier. However, the flask containing the adsorbent-dye mixture was agitated in a water bath (Heizbad HB, Heidolph, Germany) set at a predetermined temperature. The rate of removal of AB40 by TLLP was monitored at various temperatures (298, 303, 308, 313 and 318 K) until equilibrium was attained.

Standard enthalpy ($\Delta H°$, kJ mol^{-1}), standard entropy ($\Delta S°$, kJ mol^{-1} K^{-1}), and standard free energy ($\Delta G°$, kJ mol^{-1}) were determined from the following relationships

$$\Delta G^o = \Delta H^o - T\Delta S^o \tag{17}$$

$$\Delta G^o = -RT \ln K_d \tag{18}$$

$$K_d = \frac{q_e}{C_e} \tag{19}$$

and

$$\ln K_d = \frac{\Delta S^O}{R} - \frac{\Delta H^O}{RT} \tag{20}$$

where, R is the gas constant (8.314 J mol^{-1} K^{-1}), T (K) is temperature, K_d is the distribution coefficient, q_e (mg g^{-1}) is the quantity of adsorbate removed at equilibrium and C_e (mg L^{-1}) is the quantity of adsorbate remaining in solution at equilibrium. Equation (16) was used to determine the values of $\Delta G°$ at various temperatures. The values of $\Delta H°$ and $\Delta S°$ were estimated from the plot of $\ln K_d$ versus T^{-1}.

2.6. Quality Assurance and Error Analysis

Each experiment was carried out at least thrice to ensure the accuracy, reliability and reproducibility of the experimental data [35]. Any experimental value that did not fall within 5% of the mean value was rejected. The

concentration of two standard AB40 dye solutions (50 mg L^{-1} and 125 mg L^{-1}) were measured after every four or five determinations to ensure the reliability of the entire process.

The validity of the adsorption isotherm and kinetic data employed was evaluated using the correlation coefficient (R^2) obtained directly from the microsoft excel plots; together with the root mean square error (RMSE) calculated thus:

$$RMSE = \sqrt{\frac{1}{n-1}\sum_{n-1}^{n}\left(q_{e,\exp}-q_{e,cal}\right)^2} \tag{21}$$

where $q_{e,\exp}$ (mg g^{-1}) is the experimental adsorption capacity, $q_{e,cal}$ (mg g^{-1}) is the adsorption capacity predicted by the model and n is the number of data points.

Table 1: Maximum monolayer adsorption capacities of selected adsorbents for removal of AB40

Adsorbent	qm (mg g^{-1})	Reference
Teak leaf litter powder	80.64	This study
Calcinedalunite	212.80	[18]
Punicagranatum L. peels	138.10	[17]
Thujaorientalis biomass	97.06	[14]
Granular activated carbon	57.47	[18]
Chemically modified barley straw	51.95	[16]
Surfactant modified barley straw	47.60	[15]
Titania	23.70	[37]

3. Results and discussion

3.1. Equilibrium Adsorption

The contact time required for adsorption to attain equilibrium was influenced by the initial concentration of dye solution. Figure 1(a) shows that, dye solution of concentrations 25, 50 and 75 mg L^{-1} required about 100, 140 and 300 min, respectively to attain equilibrium. The rapid removal of the dye at the initial stage is due to the presence of large number of free sites on the surface of TLLP that the dye anions could attach to. The rate of uptake of dye was slow in the second stage because of substantial decrease in the number of unoccupied sites. Furthermore, repulsion between dye anions at the AB40 solution-TLLP interface was likely after all the sites on the adsorbent surface have been occupied.

The changes in the dose of TLLP used to remove AB40 from solution influence the quantity of dye removed substantially. Figure 1(b) reveals that AB40 adsorbed rose from 36% to 88% when the TLLP dosage was increased from 1 to 10 g L^{-1}. On the other hand, actual mass of dye removed plunged from 18 mg g^{-1} to 4 mg g^{-1} for the same variation in adsorbent dosage. This is attributable to fast superficial attachment of AB40 anions on TLLP adsorption sites leaving some sites vacant, possible aggregation of adsorbent particles as dosage increased preventing some sites on the adsorbent from having easy interaction with AB40 anions in solution; and possible desorption of weakly attached dye anions from the adsorbent by other adsorbent particles [36].

The effect of pH of dye solution on removal of AB40 by TLLP is presented in Figure 1(c). Removal of dye anions by the adsorbent was inversely proportional to the pH; the lower the pH, the higher the quantity of dye removed. The quantity of dye removed dropped sharply from pH 1 to pH 5 and then declined slowly between pH 5 and pH 11. This observation was due to electrostatic interaction between the positively charged binding sites on the surface of the adsorbent and the AB40 anions at low pH. The scale of positive charge on the surface of the adsorbent decreased as pH increased and, hence, the reduction in the electrostatic interaction between the adsorbent and the dye anions [14].

The uptake of AB40 from aqueous solution by TLLP was preferred at low temperatures as presented in Figure 1(d). The quantity of dye removed decreased from 39.38 mg g^{-1} to 36.48 mg g^{-1} when temperature was raised from 298 K to 313 K. This observation might be due to the weakening of bond strength between AB40 anions and the binding sites on the adsorbent. The adsorption process was exothermic in nature [14].

3.2. Adsorption Isotherm

Adsorption isotherm models are employed to define the interaction between an adsorbate and an adsorbent. This is employed to estimate the capacity of the adsorbent as well as guides to design appropriate adsorption system [38]. The adsorption equilibrium data was best described by the Langmuir isotherm (R^2 = 0.999) presented in Figure 2(a). The monolayer adsorption capacity of TLLP was found to be 80.64 mg g^{-1} while the value of R$_L$ was

0.072 signifying favorable adsorption. The monolayer capacity of TLLP for removal of AB40 is compared with the maximum monolayer capacities of other adsorbents in Table 1.

Table 2: Isotherm constants for the removal of AB40 by TLLP

Langmuir Isotherm	K_L (L mg^{-1})	q_m (mg g^{-1})	R_L	R^2	RMSE
	0.086	80.645	0.072	0.999	0.114
Scatchard Isotherm		q_m (mol g^{-1})	b (L mol^{-1})	R^2	RMSE
		1.664 x 10^{-4}	44.059	0.979	0.336
Freundlich Isotherm		K_F (mg g^{-1})(L mg^{-1})$^{1/n}$	n	R^2	RMSE
		13.496	2.501	0.963	0.374
Dubinin-Radushkevich Isotherm	β (mol^2 J^{-2})	q_{DR} (mg g^{-1})	E (kJ mol^{-1})	R^2	RMSE
	1.0 x 10^{-8}	91.818	7.071	0.997	0.152

The slope of the Scatchard plot is negative as shown in Figure 2(b), implying independent interaction between AB40 and the binding sites on TLLP [14]. The straight line without deviation implies that the adsorbent was homogenous and possessed only one type of binding site [39]. The values of q_m and b were 1.66 x 10^{-4} mol g^{-1} (or 78.59 mg g^{-1}) and 4.40 x 10^4 L mol^{-1}, respectively. The Freundlich isotherm plot for the adsorption of AB40 onto TLLP is shown in Figure 2(c). The values of K_F and n were 13.50 (mg g^{-1})(L mg^{-1})$^{1/n}$ and 2.501, respectively indicating favourable adsorption. The maximum capacity of TLLP and the mean adsorption free energy, E, produced from Dubinin-Radushkevich isotherm in Figure 1(d) were as 91.82 mg g^{-1} and 7.07 kJ mol^{-1}, respectively. The adsorption was, therefore, physical in nature because E is lesser than 8.00 kJ mol^{-1} [33]. The parameters, constants and correlation coefficients (R^2) obtained from the four isotherm models are summarized in Table 2.
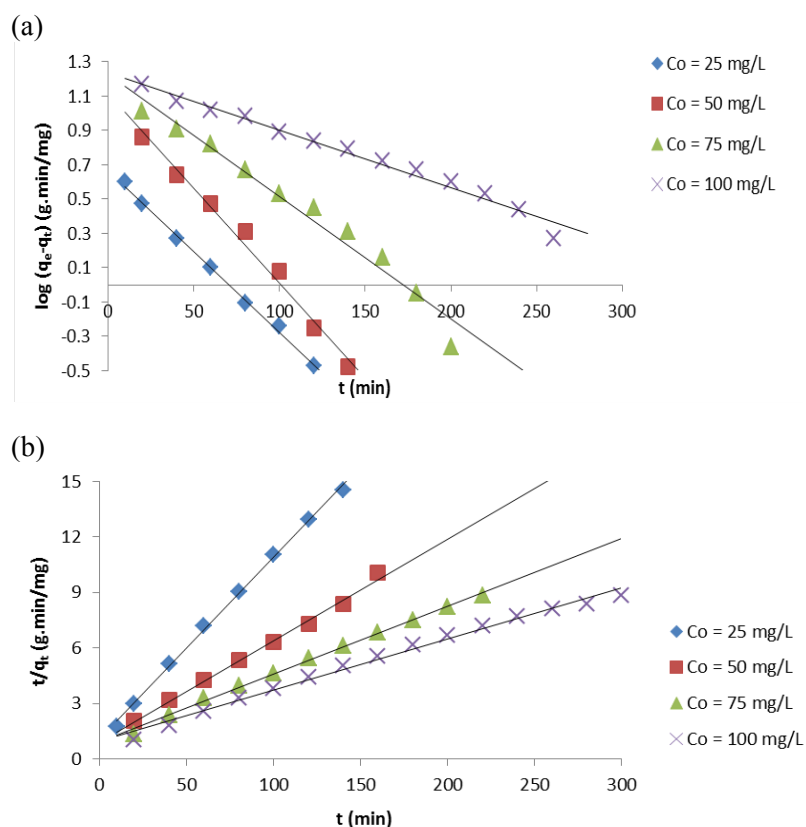
Figure 3: Pseudo-first order (a) and pseudo-second order (b) kinetic plots for removal of AB40 by TLLP

3.3. Adsorption Kinetics
Adsorption kinetics data are used to understand the mechanism of the removal of an adsorbate by an adsorbent and how to exploit it for commercial application [40]. The linear plots of pseudo-first order and pseudo-second order kinetics at 303 K are shown in Figure 3. The correlation coefficients (R^2) of the pseudo-second order plots were generally higher than 0.990 and the calculated values of q_e were close to the experimentally determined

values. On the other hand, although the correlation coefficients of the pseudo-first order plots were generally better than 0.970, the calculated values of q_e were inconsistent with those obtained from the actual kinetic experiments. Therefore, the pseudo-second order model suits the kinetic data better.

(a)

(b)
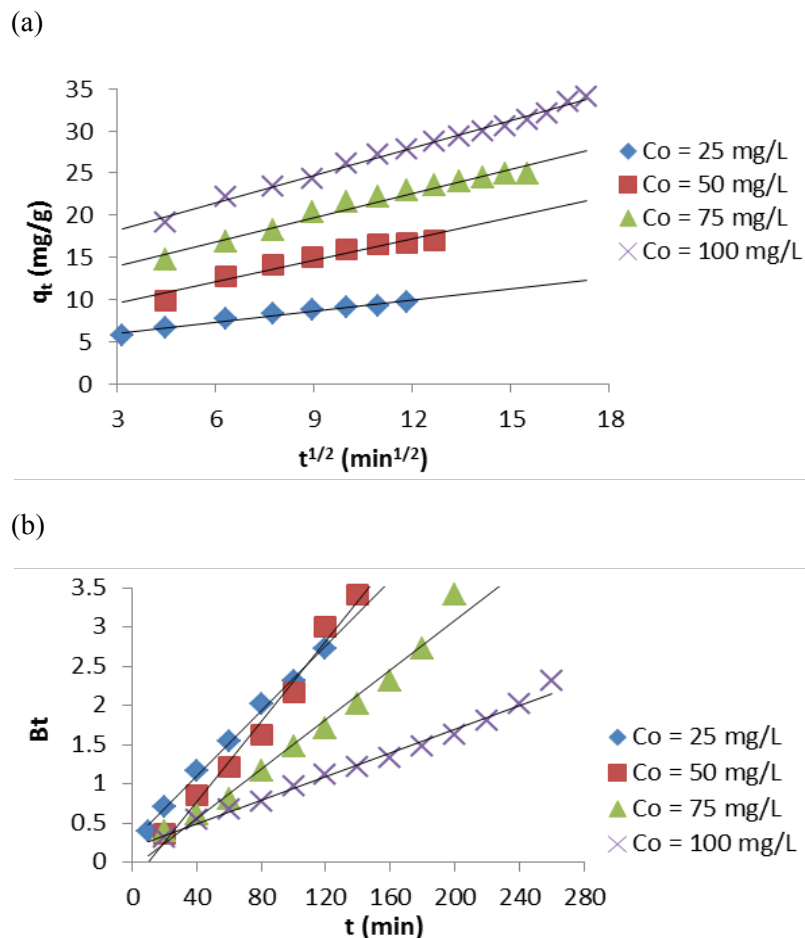
Figure 4: Intraparticle diffusion (a) and liquid film diffusion (b) kinetic plots for removal of AB40 by TLLP

Table 3: Kinetic constants for removal of AB40 from aqueous solution by TLLP

Kinetic Model	Co (mg g^{-1})			
	25	50	75	100
Pseudo-First Order				
$q_{e,cal}$ (mg g^{-1})	4.065	13.10	16.93	17.30
qe,exp (mg g^{-1})	9.62	17.06	24.93	33.99
k_1 (g mg^{-1} min^{-1})	0.022	0.026	0.016	0.008
R^2	0.997	0.987	0.970	0.982
RMSE	1.091	1.234	1.422	1.310
Pseudo-Second Order				
$q_{e,cal}$ (mg g^{-1})	10.16	18.18	27.32	36.10
$q_{e,\ exp}$ (mg g^{-1})	9.62	17.06	24.93	33.99
k_2 (g mg^{-1} min^{-1})	0.009	0.003	0.001	0.001
h (mg g^{-1} min^{-1})	0.930	1.091	1.045	1.043
R^2	0.998	0.995	0.997	0.991
RMSE	1.246	1.332	1.274	1.450
Intraparticle Diffusion				
K_{id} (mg g^{-1} min$^{-1/2}$)	0.435	0.851	0.952	1.083
C (mg g^{-1})	4.405	6.963	11.16	14.91
R^2	0.962	0.851	0.972	0.993
RMSE	1.294	1.374	1.345	0.721

The intraparticle diffusion plots were employed to elucidate the mode of diffusion of AB40 into TLLP (Figure 4). The plots were linear with correlation coefficient between 0.950 and 0.993. The intraparticle diffusion was not the rate-determining step because the plots did not pass through the origin. This suggests the involvement of boundary layer effect or liquid film diffusion on the process [40, 41]; and the higher the initial concentration of the dye solution, the larger the boundary layer effect.

The Boyd kinetic equation was applied to ascertain the actual rate-controlling step between intraparticle diffusion and liquid film diffusion. The plots shown in Figure 4(b) were linear at every initial concentration of AB40 solution. The plots did not pass through the origin. Therefore, the rate-controlling step might be by liquid film diffusion [36]. The kinetic constants for removal of AB40 from aqueous solution by TLLP are summarised in Table 3.

3.4. Adsorption Mechanism
The adsorption of AB40 onto TLLP was favoured at low pH. The mechanism of adsorption might be due to the electrostatic attraction between the positively charged surface of the adsorbent, protonated by the excess H^+ ions; and AB40 dye ion, which was negatively charged. The formation of hydroxide species, OH^-, was favoured at higher pH values. Therefore, the surface of the adsorbent would become less protonated as pH increases leading to lesser attraction of the dye ions by the adsorbent. This mechanism has been extensively discussed and the proposed equations of the process documented [42-44].

TLLP surface may be represented as ROH, where R is the matrix. At low pH values, the surface of the adsorbent may be presented as ROH_2^+, while at high pH values the surface of the adsorbent becomes deprotonated represented as RO^-. The proposed equations at low pH values are:

$$ROH + H^+ \longrightarrow ROH_2^+ \tag{22}$$
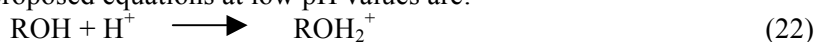
The negatively charged dye ion, represented as $AB40^-$, then couples to the adsorbent as follows:

$$ROH_2^+ + AB40^- \longrightarrow RO\text{-}AB40 + H^+ \tag{23}$$

As pH of the dye solution increases, the following reactions may occur:

$$ROH + OH^- \longrightarrow RO^- + H_2O \tag{24}$$

$$ROH_2^+ + 2OH^- \longrightarrow RO^- + 2H_2O \tag{25}$$
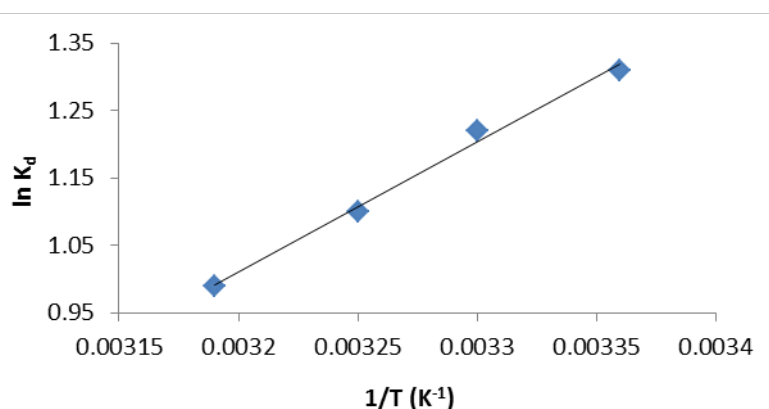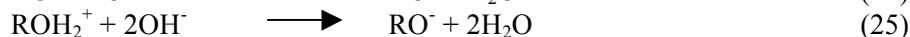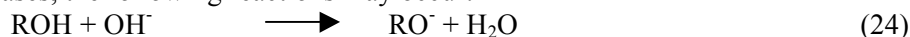
Figure 5: Plot of lnK_d versus $1/T$ for estimating the values of thermodynamic parameters

Table 4: Values of thermodynamic parameters for removal of AB40 from aqueous solution by TLLP

	$\Delta G°$ (kJ mol^{-1})			$\Delta H°$ (kJ mol^{-1})	$\Delta S°$ (J mol^{-1} K^{-1})
298 K	303 K	308 K	313 K		
-3.25	-3.08	-2.83	-2.58	-15.99	-42.77

3.5. Adsorption Thermodynamics
The plot of lnK_d against $1/T$ is presented in Figure 5. The values of $\Delta G°$, $\Delta H°$ and $\Delta S°$, the thermodynamic parameters, are collated in Table 4. The negative values of $\Delta G°$ at the range of temperature studied suggested that the adsorption process was spontaneous and thermodynamically favorable. The negative value of $\Delta H°$

confirmed the exothermic nature of the process [14]. The negative value of $\Delta S°$ (-42.77 J mol^{-1}) reflected the reduced randomness at the TLLP-AB40 solution interface [45].

Conclusion

TLLP was prepared from abundant but disregarded TLL as a low-cost adsorbent for removing AB40 from aqueous solution. The adsorbent possessed low activity level due to the combination of its low surface area and low iodine number. However, optimum removal of the dye occurred at low TLLP dosage, acidic pH, and low dye concentration. The contact time required for adsorption to attain equilibrium was proportional to the initial concentration of dye solution. Electrostatic interaction between the positively charged binding sites on the surface of TLLP and the AB40 anions were mainly responsible for the removal of the dye from aqueous solution by the adsorbent.

Langmuir isotherm model best fit the equilibrium adsorption data at 303 K. The maximum monolayer capacity of TLLP as adsorbent for AB40 was 80.64 mg g^{-1}. The adsorbent was homogenous with only one type of binding site. There was an independent interaction between the dye and the binding sites on the adsorbent. The adsorption process was best described by pseudo-second order kinetic model at 303 K. Boundary layer diffusion played some role in the adsorption process. The mechanism of adsorption might be due to the electrostatic attraction between the positively charged surface of the adsorbent and negatively charged AB40 dye ion. The uptake of AB40 by TLLP was influenced by both liquid film diffusion and intraparticle diffusion but the latter was the rate controlling step. The process was spontaneous, thermodynamically feasible and exothermic. The values of change in standard enthalpy and mean adsorption free energy suggest that the process was physical adsorption. TLLP has potential to be used as a low-cost adsorbent for treating wastewaters contaminated by AB40.

References

1. S.H. Lin, R.S. Juang, Y.H. Wang, *J. Hazard. Mater*. 113 (2004) 195-200.
2. S-T. Ong, P-S. Keng, W-N. Lee, S-T. Ha, Y-T. Hung, *Water* 3 (2011) 157–176.
3. M. Ejder-Korucu, A. Gürses, Ç. Doğar, S.K. Sharma, M. Açıkyıldız, in: S.K. Sharma (Ed*.), Green Chemistry for Dyes Removal from Wastewater*, Scrivener Publishing LLC, Salem, MA, 2015, pp. 1-22.
4. C. Namasivayam, R. Radhika, S. Suba, *Waste Manag*. 21 (2001) 381-387.
5. M.M. Ayad, A.A. El-Nasr, *J. Nanostruct. Chem*. 3 (2012) 1-9.
6. E. Ortiz, H. Solis, L. Noreña, S. Loera-Serna, *Int. J. Environ. Sci. Dev*. 8(4) (2017) 255-259.
7. Z. Wang, M. Xue, K. Huang, Z. Liu, in: P.J. Hauser (Ed.) *Advances in Treating Textile Effluent*, InTech, 2011, pp. 91-116.
8. A. shfaq, A. Khatoon, Int. J. Curr. Microbiol. *Appl. Sci*. 3(7) (2014) 780-787.
9. M.T. Yagub, T.K. Sen, S. Afroze, H.M. Ang, *Adv. Colloid Interface Sci*. 209 (2014) 172–184.
10. S. Kanchi, K. Bisetty, G. Kumar, M.I. Sabela, *Arab. J. Chem*. 10(S2) (2017) S3087-S3096.
11. Y. Zhang, Z. Zhou, Y. Shen, Q. Zhou, J. Wang, A. Liu, S. Liu, Y. Zhang, *ACS Nano* 10(9) (2016) 9036-9043.
12. A.S. Angelatos, K. Katagiri, K. F. Caruso, *Soft Matter* 2 (2006) 18-23.
13. L. Hartmann, M. Bedard, H.G. Boerner, H. Moehwald, G.G. Sukhorukov, M. Antonietti, *Soft Matter* 4 (2008) 534-539.
14. T. Akar, A.S. Ozcan, S. Tunali, A. Ozcan, *Bioresour. Technol*. 99 (2008) 3057-3065.
15. B.C. Oei, S. Ibrahim, S. Wang, H.M. Ang, *Bioresour. Technol*. 100 (2009) 4292-4295.
16. S. Ibrahim, I. Fatimah, H-M. Ang, S. Wang, *Water Sci. Technol*. 62(5) (2010) 1177-1182.
17. Ç.Ö. Ay, A.A. Özcan, Y. Erdoğan, A. Özcan, *Colloids Surf. B: Biointerfaces* 100 (2012) 197-204.
18. M. Özacar, A. Şengil, *Adsorpt*. 8 (2002) 301-308.
19. E.O. Oyelude, J.A.M. Awudza, S.K. Twumasi, *Sci. Rep*. 7 12198 (2017) 1-10. DOI: 10.1038/s41598-017-12424-1.
20. D. Verhaegen, I.J. Fofana, Z.A. Logossa, D. Ofori, *Tree Genetics and Genomes* 6 (2010) 717-733.
21. H. Purnomo, P. Guizol, P. D.R. Muhtaman, *Environ. Model. Softw*. 24 (2009) 1391-1401.
22. G.D. Djagbletey, S. Adu-Bredu, *Ghana J. For*. 20 and 21 (2007) 1-13.
23. A.K.N. Aoudji, A. Adégbiji, S. Akoha, V. Agbo, V. P. Lebaily, *Tropicultura* 30(1) (2012) 55-60.
24. A.F. Ojo, T.O.S. Kadeba, J. Kayode, *Bangladesh J. Sci. Industrial Res*. 45(4) (2010) 351-358.
25. L. Langmuir, *J. Am. Chem*. Soc. 40 (1918) 1361-1403.
26. G. Scatchard, *Annals N. Y. Academy Sci*. 51 (1949) 660-672.
27. H.M.F. Freundlich, *J. Phys. Chem*. 57 (1906) 385–470.

28. M.M. Dubinin, L.V. Radushkevich, *Proc. Academy Sci., Phys. Chem. Sect.; USSR* 55 (1947) 331-333.
29. S. Lagergren, *K. Sven. Vetensk. Akad. Handl*. 24 (1898) 1-39.
30. N. Gupta, A.K. Kushwaha, M.C. Chattopadhyaya, *J. Taiwan Inst. Chem. Eng*. 43 (2012) 604-613.
31. Y.S. Ho, G. McKay, *Process Biochem*. 34 (1999) 451-465.
32. W.J. Weber, J.C. Morris, *J. Sanit. Eng. Div. Am. Soc. Civ. Eng*. 89 (1963) 53-61.
33. S.S. Gupta, K.G. Bhattacharyya, *Adv. Colloid Interface Sci*. 162 (2011) 39-58.
34. G.E. Boyd, A.W. Adamson, L.S. Meyers Jr., *J. Am. Chem. Soc*. 69(11) (1947) 2836-2848.
35. M.C. Ribas, M.A. Adebayo, L.D.T. Prola, E.C. Lima, R. Cataluna, L.A. Feris, M.J. Pochana-Rosero, F.M. Machado, F.A. Pavan, T. Calvete, Chem Eng. J. (2014). DOI: http://dx.doi.org/10.1016/j.cej.2014.03.054.
36. D.Uzunoğlu, A. Özer, *Desalination Water Treat*. 57(30) (2016) 14109-14131.
37. M.L. Fetterolf, H.V. Patel, J.M. Jennings, *J. Chem. Eng. Data* 48(4) (2003) 831-835.
38. H. Javadian, F. Ghorbani, H-A. Tayebi, S.M. Asl, *Arab. J. Chem*. 8 (2015) 837-849.
39. T.S. Anirudhan, P.S. Suchithra, *Industrial J. Chem. Technol*. 17 (2010) 247-259.
40. W. Ma, X. Song, Y. Pan, Z. Cheng, G. Xin, B. Wang, X. Wang, *Chem. Eng. J*. 193-194 (2012) 381-390.
41. Y. Liu*, J. Chem. Eng. Data* 54 (2009) 1981-1985.
42. S. Inan, Y. Atlas *Sep. Sci. Technol.* 45 (2010) 269-276.
43. K. Kumar, H.B. Yogesh, Y. Muralidhara, N. Arthoba, J. Balasubramanyam, H. Hanumanthappa*Powder Technol*. 239 (2013) 208-216.
44. R.A.K. Rao, U. Khan, *Groundw. Sustainable Dev.* 5 (2017) 244-252.
45. X-F. Sun, S-G. Wang, X-W. Liu, W-X. Gong, N. Bao, B-Y. Gao, H.Y. Zhang, *Bioresour. Technol*. 99 (2008) 3475-3483.

(2018) ; http://www.jmaterenvironsci.com